processes

Article

Application of Micro-Seismic Monitoring in Post-Fracturing Evaluation of Shale Gas: A Case Study of Well X from Puguang Area, China

Lufeng Zhang [1,2,*], Haibo Wang [1,2], Jiujie Cai [1] and Shicheng Zhang [3,*]

[1] Key Laboratory of Marine Oil & Gas Reservoirs Production, Sinopec Petroleum Exploration and Production Research Institute, Beijing 100083, China; wanghaibo.syky@sinopec.com (H.W.); caijj.syky@sinopec.com (J.C.)
[2] State Energy Center for Shale Oil Research and Development, Beijing 100083, China
[3] China University of Petroleum-Beijing, Beijing 100083, China
* Correspondence: zlfcupb@163.com (L.Z.); zhangsc@cup.edu.cn (S.Z.)

Abstract: Multi-stage fracturing of horizontal wells is an indispensable technology to create complex fracture networks, which can unlock production potential and enable commercial productivity for shale gas with low porosity and permeability. Real-time monitoring of fracture networks is essential for adjusting key parameters, mitigating fracturing risks, and achieving optimal fracturing effects. Micro-seismic monitoring technology accurately captures and describes the development of fracture networks by detecting micro-seismic waves generated through rock ruptures, providing valuable insights into the evaluation of post-fracturing. In this study, we first introduced the basic parameters of well X that were obtained by laboratory experiments and logging interpretation, including porosity, gas-bearing properties, mineral composition, rock mechanics, and crustal stress. Then, the hydraulic fracturing scheme was designed on the basis of the geological engineering characteristics of well X. Finally, we conducted a comprehensive analysis of various factors that can affect hydraulic fracturing. This included an examination of the impact of pre-fluid temporary plugging and fracture complexity on the overall effectiveness of the operation. Based on the laboratory experiments and theoretical analysis, the following conclusions can be drawn: (1) fracture size is essentially formed when the fluid strength exceeds 35 m^3/m; (2) both preflush with high viscosity and the amount of power sand exceeding 20 cubic meters are conducive to the propagation of fracture height; (3) temporary plugging balls facilitate the balanced propagation of multiple fracture clusters within a stage, whereas temporary plugging particles promote the formation of complex fractures; and (4) geological conditions are a prerequisite for creating a complex network of fractures, and only engineering techniques can facilitate the appropriate enhancement of fracture complexity. This study provides an essential method for the fracturing design of shale gas.

Keywords: multi-stage fracturing; shale gas; micro-seismic monitoring; fracture network

check for updates

Citation: Zhang, L.; Wang, H.; Cai, J.; Zhang, S. Application of Micro-Seismic Monitoring in Post-Fracturing Evaluation of Shale Gas: A Case Study of Well X from Puguang Area, China. *Processes* **2023**, *11*, 1863. https://doi.org/10.3390/pr11071863

Academic Editor: Qingbang Meng

Received: 22 May 2023
Revised: 17 June 2023
Accepted: 18 June 2023
Published: 21 June 2023

Copyright: © 2023 by the authors. Licensee MDPI, Basel, Switzerland. This article is an open access article distributed under the terms and conditions of the Creative Commons Attribution (CC BY) license (https://creativecommons.org/licenses/by/4.0/).

1. Introduction

The U.S. Energy Information Administration (EIA) has recently released the Annual Energy Outlook 2022, which states that the majority of production increases since the turn of the 21st century can be attributed to the use of horizontal drilling and hydraulic fracturing techniques [1]. These methods have been particularly effective in unlocking reserves from tight geologic formations such as shale [2–5]. However, there are various challenges due to the complex and dynamic stress state, strong anisotropy and heterogeneity of rock mechanics properties, unclear development of natural fractures, and interference between artificial fractures during the hydraulic fracturing of unconventional reservoirs [6,7]. As a result, the actual hydraulic fractures that are formed often differ significantly from the design plan in terms of their distribution, fracture length, shape, and proppant filling.

Moreover, the uniformity of artificial fractures formed by multi-stage fracturing in horizontal wells is often poor, with only 1/3 to 1/2 of the perforated clusters being effectively stimulated [8–10]. Therefore, improving the accuracy of hydraulic fracturing evaluation has become a critical technology for solving the bottleneck problem of unconventional resource development.

To evaluate the effectiveness of post-fracturing, commonly used methods include micro-seismic imaging, fiber optic monitoring, conductive fracture-imaging technology, and so on [10–14]. Micro-seismic monitoring is a direct measurement method for determining the geometric parameters of fractures. It can image the size and shape of hydraulic fractures while observing their propagation mode. Through monitoring the small vibrations generated by rock fractures during hydraulic fracturing, micro-seismic monitoring technology can determine the location and timing of rock fractures. It analyzes the rock activity and state of the target layer and can be used to guide real-time improvements in fracturing technology and evaluate fracturing effectiveness [15,16]. This technology is widely used in shale gas hydraulic fracturing processes.

In light of this, many scholars have conducted extensive research on interpreting micro-seismic monitoring results and using them to evaluate hydraulic fracturing effectiveness. Based on radial-array micro-seismic monitoring technology, the optimization of preflush parameters, perforation, and the delivery time of temporary plugging agents was guided in real time. This led to an average 2- to 5-fold increase in shale gas production during testing, which improved the fracturing effect [17]. Wang et al. [18] accurately analyzed parameters such as the propagation area and length of newly opened fractures during re-fracturing of old wells. Real-time adjustments were made to displacement, sand volume, and delivery timing of temporary plugging materials, resulting in a post-fracturing production rate that was 4 to 5 times higher than before re-fracturing. Using 3D seismic and logging data to characterize reservoir characteristics, Zhao et al. analyzed the spatial distribution and seismic attributes of micro-seismic events and conducted field applications [11,19]. Currently, micro-seismic monitoring is mainly applied to guide hydraulic fracturing and verify the reliability of artificial fracture prediction methods, but there is no complete technical process based on micro-seismic monitoring for evaluating the post-fracturing effects.

The structure of this paper is as follows. Firstly, we introduced the basic parameters of well X that were obtained by laboratory experiments and logging interpretation, including porosity, gas-bearing properties, mineral composition, rock mechanics, and crustal stress. Then, the hydraulic fracturing scheme was designed on the basis of the geological engineering characteristics of well X. Finally, we conducted a comprehensive analysis of various factors that can affect hydraulic fracturing. This included an examination of the impact of pre-fluid temporary plugging and fracture complexity on the overall effectiveness of the operation. This study provides an essential method for the fracturing design of shale gas.

2. Evaluation of Geological Engineering Parameters

Well X is a horizontal well situated in the Puguang area of the Sichuan Basin in China and is primarily aimed at exploring the *Dalong* layer. The target depths for target A and target B are 4565 m and 5800 m, respectively, and the total length of the horizontal section is 1235 m. As shown in Figure 1, the analysis of seismic curvature attributes reveals the presence of weak stratigraphic planes within the horizontal section at depths of 4565–4651 m and 4865–4968 m, indicating that the natural fractures are well developed.

The geological engineering parameters for well X are determined through logging interpretation and laboratory experiments and include porosity, gas-bearing properties, mineral content, rock mechanics parameters, and crustal stress. The methods used for calculation were conventional methods for well logging interpretation. These parameters provide the essential data required for evaluating the effectiveness of post-fracturing operations.

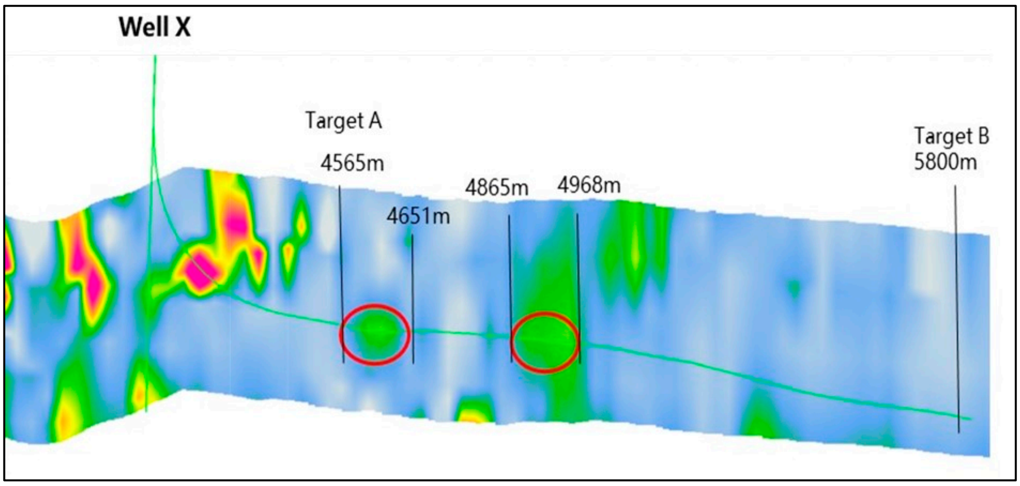

Figure 1. Distribution of curvature attributes along horizontal well sections of well X.

2.1. Porosity

Porosity is the basic parameter of a reservoir which determines its storage and seepage capacity. Furthermore, it also has a certain impact on the selection of fracturing technology, such as the selection of fracturing fluids. Therefore, porosity is of great significance for improving hydrocarbon recovery after hydraulic fracturing.

According to the logging interpretation, the distribution of porosity for the entire horizontal section is shown in Figure 2. It can be seen that the porosity of the horizontal section ranges from 0.62% to 4.93%, with an average of 2.61%. The porosity in the middle and front parts is relatively high, which is related to the development of micro-fractures. Overall, the porosity of the horizontal section for well X is relatively low, and tight-closed volume fracturing may be needed to form an artificial complex fracture net in order to improve the underground hydrocarbon-seepage capacity.

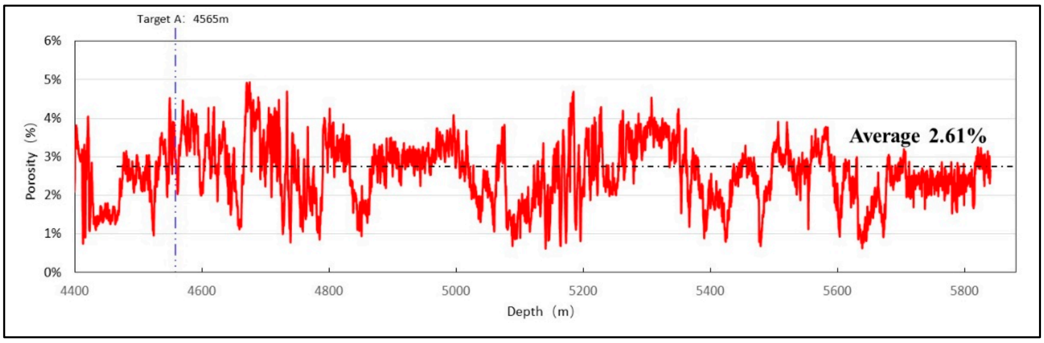

Figure 2. Distribution of porosity for the entire horizontal well section.

2.2. Gas-Bearing Properties

Reservoir gas-bearing refers to the ratio of the volume of gas contained in pores or fractures a in reservoir to the total volume of the reservoir. It is an important physical property that reflects the gas-storage capacity of the reservoir. Moreover, free gas refers to gas that has not formed a dissolved or adsorbed state and exists in the pores of the reservoir. Free gas occupies the pore volume and can flow and increase the gas phase pressure of the reservoir or wellbore. In the process of oil exploration and development, free gas is an important concept because it not only determines the exploration value of oil and gas reservoirs, but also has a significant effect on production capacity after hydraulic fracturing.

According to the logging interpretation, the distribution of gas-bearing and free gas proportions for the entire horizontal section is shown in Figure 3. It can be seen that gas content in the horizontal section is 0.45–11.16 m^3/t, with an average of 5.14 m^3/t. Furthermore, the free gas content is 0.001–7.34 m^3/t, with an average of 3.55 m^3/t, and the free gas proportion is 15.7–99.8%, with an average of 71.58%. Overall, the content of free gas is relatively high, which is conducive to achieving high production after hydraulic fracturing.

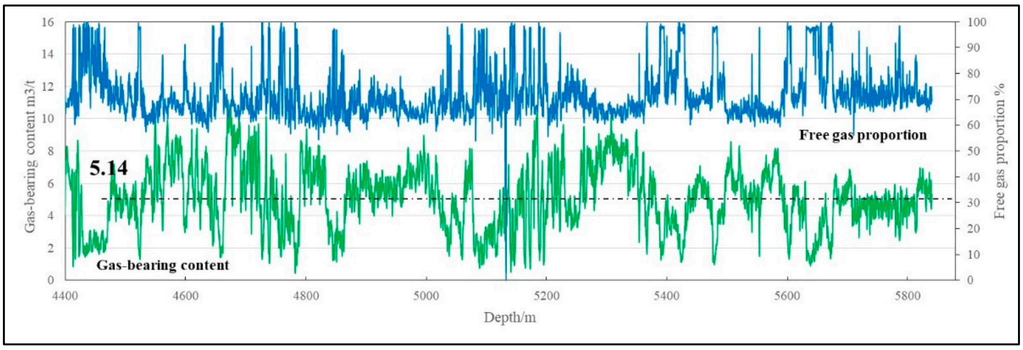

Figure 3. Distribution of gas-bearing and free gas proportions for the entire horizontal well section.

2.3. Mineral Composition

The mineral composition of the reservoir has a significant effect on the mechanical properties of the rocks, fracability evaluation of the formation, and effectiveness of fracturing fluids. For example, a high content of clay minerals can lead to strong reservoir plasticity, making it difficult to create complex fracture networks, and the migration and expansion of clay minerals can cause reservoir damage, which requires higher fracturing fluid requirements.

According to the logging interpretation and XRD experiments, the distribution of mineral composition for the entire horizontal section is shown in Figure 4. It can be seen that the main minerals for the horizontal section are composed of clay, silica, and calcium. Moreover, both XRD experiments and logging interpretation show that silica and calcium are the main minerals, constituting over 80% of mineral content, and that the proportion of clay minerals is less than 20%. In general, engineering design is based on experimental data. Therefore, the average content of clay, silica, and calcium is approximately 4.28%, 46.49%, and 39.64%, respectively. Overall, due to a high brittle minerals content, the target well is suitable for hydraulic fracturing to form complex fracture networks from the perspective of mineral composition alone.

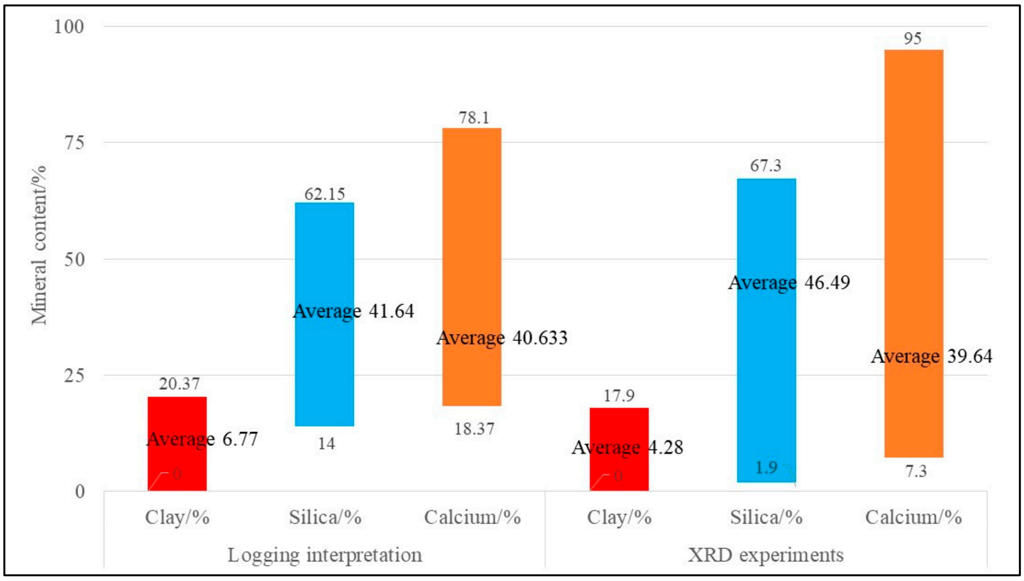

Figure 4. Comparative analysis of mineral composition for target formation.

2.4. Rock Mechanics Parameters

Rock mechanics parameters are mainly used to describe the deformation and fracture behavior of rocks under external force, including tensile strength, compressive strength, Young's modulus, Poisson's ratio, etc. In addition, these parameters mainly determine the fracture initiation, fracture propagation, and final fracture morphology during hydraulic fracturing.

According to the laboratory experiments, the measured parameters of different rock mechanics are shown in Table 1. It can be seen that as the confining pressure increases, the compressive strength, Young's modulus, and Poisson's ratio all increase. Especially under high confining pressure, it exhibits high compressive strength and high Young's modulus characteristics, indicating the difficulty of fracture initiation and small fracture width of artificial fractures during hydraulic fracturing. Moreover, the measured cohesion force and internal fraction angle are relatively high at 13.12 MPa and 55.76°, respectively, further indicating the difficulty of fracture initiation and propagation. Similarly, the measured tensile strength and fracture toughness are 12.47 MPa and 0.77 MPa$\sqrt{m}$, respectively, also indicating that in the target formation it is difficult to form complex fracture networks during hydraulic fracturing.

Table 1. Rock mechanics parameters of target formation.

Well X Target Formation			
Confining pressure MPa	0	20	40
Compressive strength MPa	68.15	218.71	491.13
Young's modulus GPa	26.24	32.19	53.66
Poisson's ratio	0.21	0.26	0.34
Cohesion force MPa		13.12	
Internal friction angle °		55.76	
Tensile strength MPa		12.47	
Fracture toughness MPa$\sqrt{m}$		0.77	

2.5. Crustal Stress

Crustal stress and horizontal stress difference are the two most important parameters that affect the fracture initiation and fracture networks during hydraulic fracturing. Due to the propagation of hydraulic fractures along the direction of the maximum horizontal principal stress, the maximum horizontal principal stress determines the fracture initiation pressure. Furthermore, the horizontal stress difference determines the complexity of the artificial fracture network due to the need to overcome the horizontal stress difference to form a complex fracture network.

The three-dimensional principal stress and horizontal stress difference obtained by logging interpretation and laboratory experiments are shown in Figure 5. It can be seen that the experimental test results are essentially consistent with the logging interpretation results. The maximum horizontal principal stress and horizontal stress difference are approximately 106 MPa and 10 MPa, respectively. On the whole, this horizontal stress difference is not high in terms of deep shale gas. Moreover, the corresponding fracturing technology can overcome the horizontal stress difference and form complex artificial fracture networks.

The direction of crustal stress is an important factor affecting fracture propagation. As shown in Figure 6, the FMI logging analysis results show that drilling-induced fractures are commonly developed in the measurement section of well X, and local wellbore collapse is observed. The direction induced by drilling represents the direction of the current maximum horizontal principal stress, while the direction of wellbore collapse represents the direction of the current minimum horizontal principal stress. The current maximum horizontal principal stress of this well is in the near East–West (90°) direction, while the current minimum horizontal principal stress is in the near South–North (0°) direction.

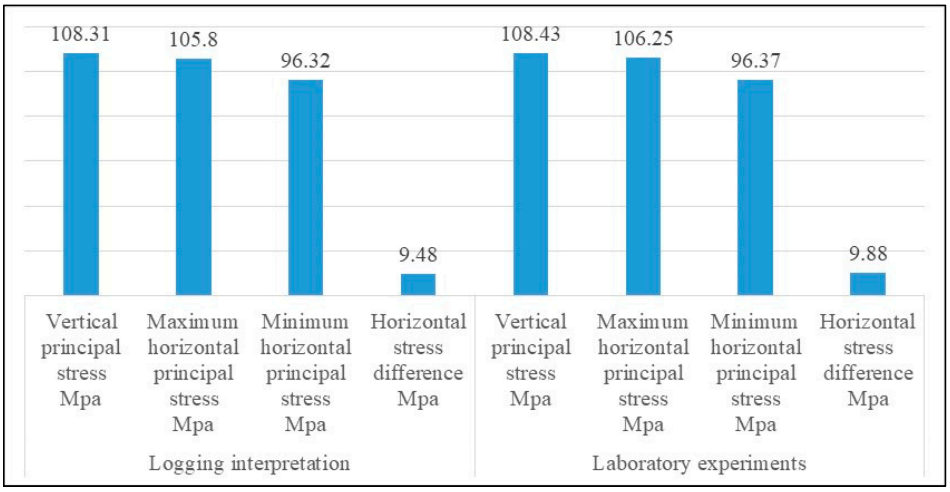

Figure 5. Crustal stress obtained by experiments and logging interpretation for target formation.

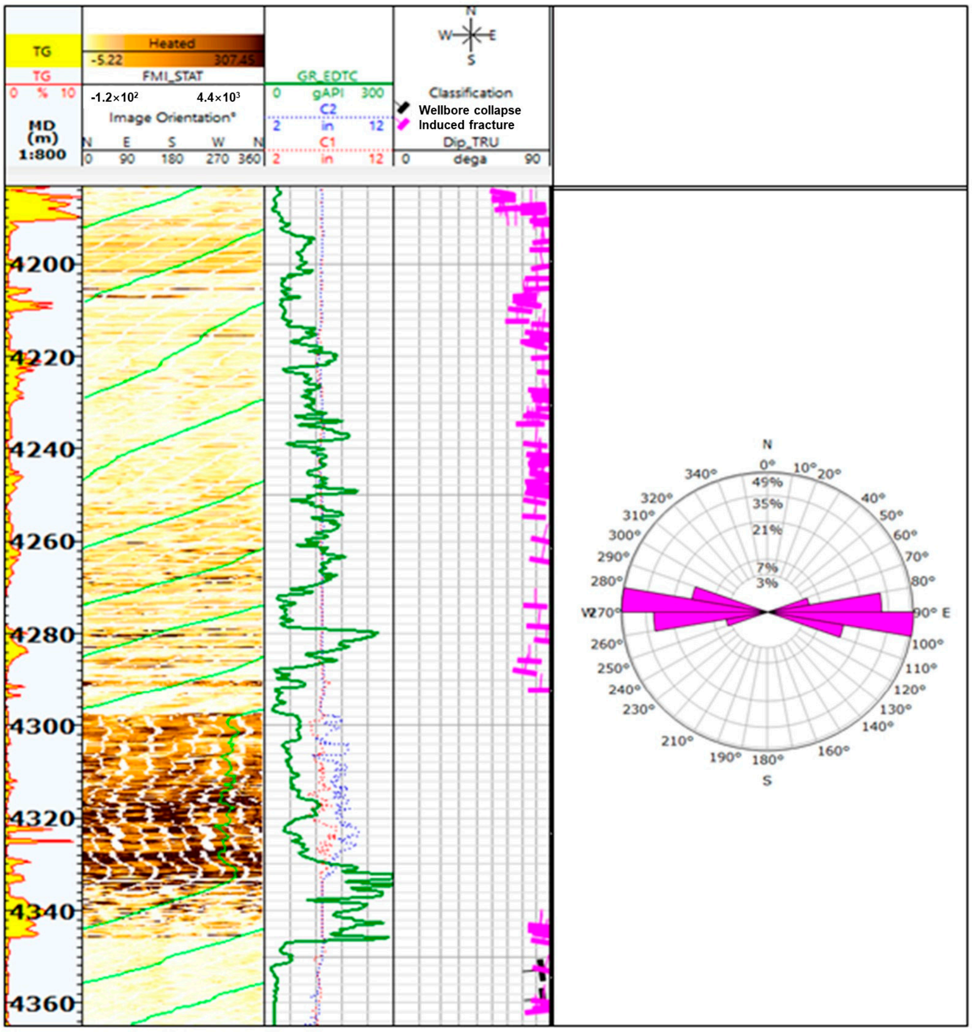

Figure 6. FMI crustal stress analysis of target well X.

3. Results and Discussion

Based on the investigation of target well X mentioned above, the hydraulic fracturing design was performed and the field practice was carried out. In addition, micro-seismic monitoring was used to evaluate the post-fracturing effect.

3.1. Hydraulic Fracturing Design and Field Application

3.1.1. Design Concept

Based on the fundamental investigation of well X by logging interpretation and laboratory experiments, the corresponding fracturing technology design was performed. Furthermore, the favorable conditions for fracturing design can be summarized as follows: (1) the thickness of high-quality shale reaches 33 m and the formation pressure coefficient is approximately 1.68, which indicates there is sufficient gas supply after hydraulic fracturing; (2) the low content of clay minerals and relatively high content of brittle minerals are conducive to forming complex fracture networks during fracturing; and (3) the small angle between the trajectory of a horizontal well and the minimum horizontal principal stress is conducive to artificial fracture propagation and increases the stimulated reservoir volume. Conversely, the unfavorable conditions for fracturing design can be summarized as follows: (1) the target formation is deeply buried, with high operation pressure and difficulty in fracture initiation; (2) the target formation with a high modulus and Poisson's ratio will result in a small fracture width during hydraulic fracturing, which makes it difficult to add proppant; and (3) the closure stress of the target reservoir is as high as 96 MPa, making it difficult for the artificial fractures to maintain high long-term conductivity after hydraulic fracturing.

In light of these favorable and unfavorable conditions, the "multi-stage with few clusters + pre high viscosity fracturing fluid + composite temporary plugging + high conductivity" large-scale fracturing concept was proposed to enhance the stimulation effect of well X. Specifically, the entire horizontal well section of well X is divided into 25 stages with an average of 45 m, and the designed average fluid strength and proppant adding strength are 55 m^3/m and 2.5 m^3/m, respectively.

3.1.2. Field Application

According to the design, the on-site fracturing operation was carried out on the target well X. The operation's wellhead pressure, pump rate, and sand ratio for stages 1 to 25 are shown in Figure 7. It can be seen that the operation's overall wellhead pressure distribution is between 96 MPa and 112 MPa and that the pump rate distribution is between 12 m^3/m and 16 m^3/m. Essentially, the wellhead pressure is close to the equipment pressure limit due to the narrow operation pressure window, which limits the increase in pump rate.

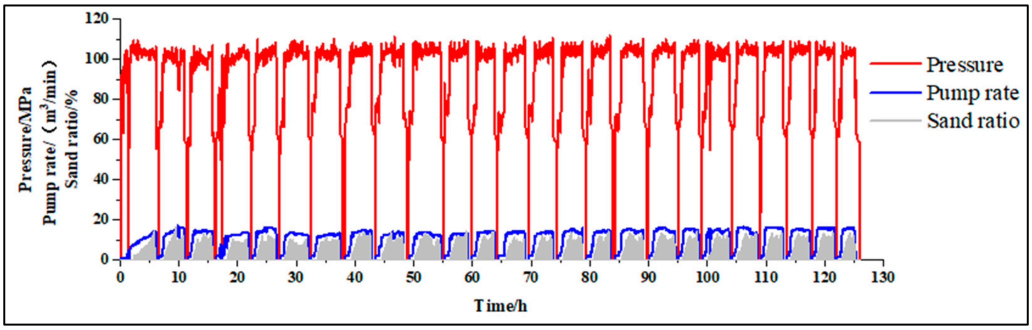

Figure 7. Operation curve of hydraulic fracturing for target well X.

Figure 8 shows the distribution of fracturing fluid and proppant for each of the 25 stages as well as the corresponding fluid and sand strength. In terms of fracturing fluids, it can be seen that a total of 75,000 cubic meters of fracturing fluid were used, including hydrochloric acid, low-viscosity slickwater, high-viscosity slickwater, and cross-linked slickwater. Among them, hydrochloric acid is mainly used for pre-fracturing to reduce rock breakdown pressure, so the dosage is relatively low. Slickwater is mainly composed of high-viscosity content, accounting for 70% to 80% of the total, while its low-viscosity and cross-linked contents are relatively low. Furthermore, the fluid strength of each stage ranges from 43 m^3/m to 75 m^3/m, with an average of 63 m^3/m. The fluid strength of well X is approximately twice that of conventional shale reservoirs, and high fluid strength is of great significance in promoting complex fracture networks.

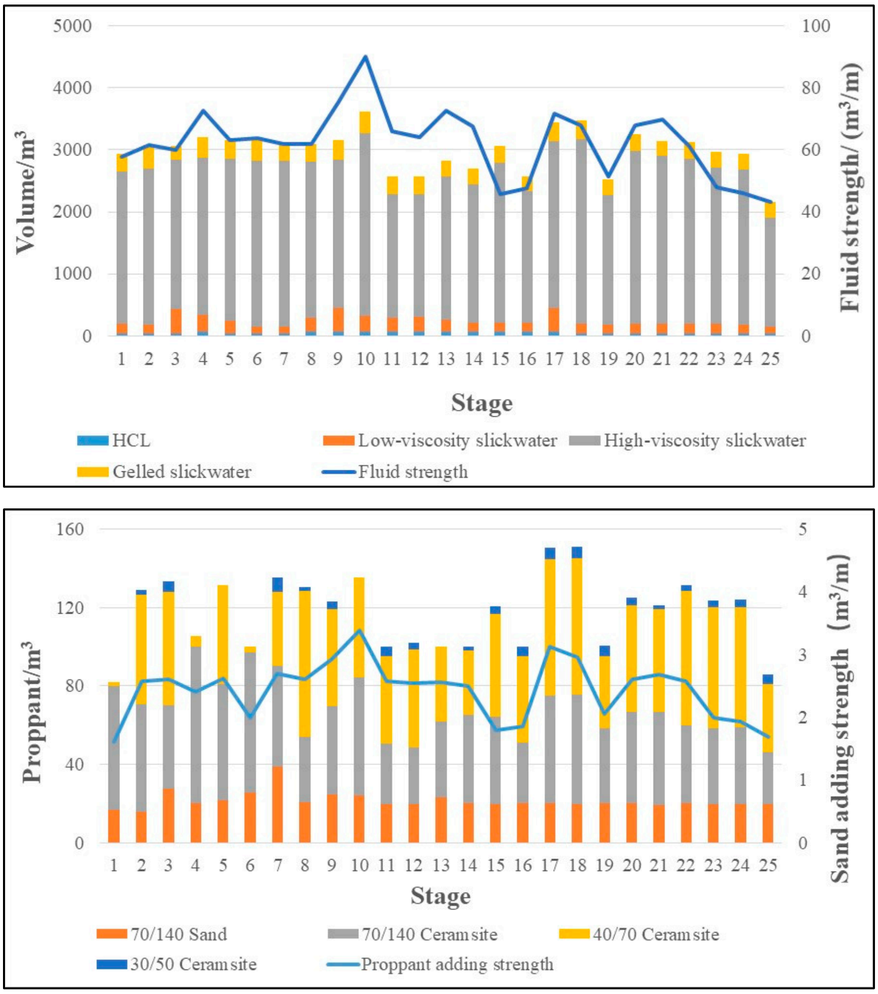

Figure 8. Fracturing fluids and proppant distribution for 25 stages of target well X.

In terms of proppant, it can be seen that a total of 2940 cubic meters were used, including 70/140 mesh quartz sand and 70/140, 40/70, and 30/50 mesh ceramsite. Among them, the quartz sand was located at the front of the operation pumping schedule, which was mainly used to polish perforation holes so as to reduce the friction of perforation holes. This can improve the operation pressure window and facilitate subsequent proppant addition. Ceramsite is mainly composed of 70/140 mesh and 40/70 mesh, accounting for approximately 80% of the total. Due to the large particle size of 30/50 mesh ceramsite, it is difficult to add during hydraulic fracturing, and only a small amount was used for fracture-mouth placement to improve long-term conductivity. Moreover, the proppant-adding strength of each stage ranges from 1.6 m^3/m to 3.4 m^3/m, with an average of 2.4 m^3/m, which is essentially equivalent to the conventional sanding strength of current shale reservoirs.

3.2. Micro-Seismic Monitoring

The distribution of ground detectors can be mainly divided into star-shaped and grid-shaped types. Compared with other micro-seismic instruments, micro-seismic ground detectors with a star-shaped distribution have advantages such as flexible point placement, high accuracy, and high sensitivity. They can capture extremely small seismic signals and quickly collect data over a large range. The use of such seismic detection equipment can provide a more accurate understanding of fracture morphology parameters and provide a scientific basis for real-time adjustment and post-fracturing evaluation of hydraulic fracturing.

As shown in Figure 9, the ground detectors of well X are mainly arranged in a star shape, with 14 receiving lines uniformly distributed in a scattered pattern around the well trajectory. The receiving point distance of each detector is 10 m. Moreover, from the distribution of micro-seismic events monitored, it can be seen that the propagation of fractures on both sides of the horizontal well section is not uniform and that hydraulic fractures mainly extend to the west.

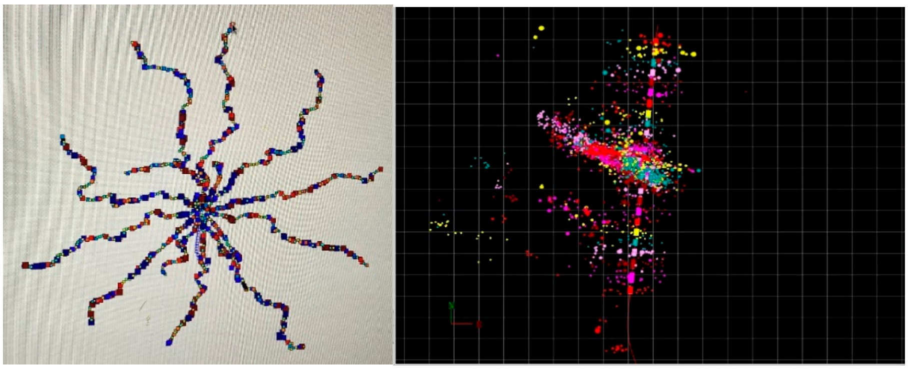

Figure 9. Ground detectors and monitored micro-seismic events distribution for target well X.

As shown in Figure 10, fracture parameters such as length, width, and height were calculated using the number of micro-seismic events observed. The results indicate that fracture length ranges from 154 m to 478 m, with the western side showing a distribution between 53 m and 378 m and the eastern side showing a distribution between 47 m and 163 m. Fracture width ranges from 53 m to 87 m, with the north side displaying a distribution between 18 m and 46 m and the south side displaying a distribution between 24 m and 62 m. Finally, fracture height distribution ranges from 25 m to 48 m, with the upper height displaying a distribution between 8 m and 23 m and the lower height showing a distribution between 10 m and 28 m. It is worth mentioning that the relationship between the number of micro-seismic events and fracture size is relatively weak when the fluid strength is high, indicating that the fracture size is mostly formed when the fluid volume exceeds a certain level.

3.3. Effect of Preflush

According to the micro-seismic monitoring events, we can calculate the artificial fracture parameters at different stages during hydraulic fracturing. As shown in Figure 11, we compared and analyzed the fracture height and total fracture height in the pre-stage due to the significant impact of the pre-stage on hydraulic fracture propagation. It can be seen that the fracture height distribution in the pre-stage is between 19 m and 41 m. The fracture height with approximately 300 m^3 of preflush in the pre-stage is approximately 71% to 93% of the total fracture height. In other words, the fractures have essentially propagated longitudinally, indicating that the cross-linked slickwater with high viscosity has a favorable effect on the propagation of the fracture height.

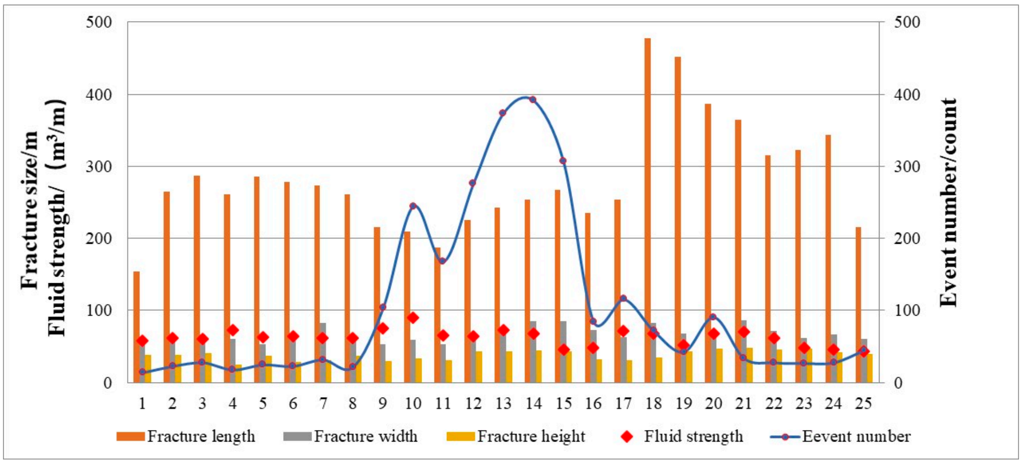

Figure 10. Monitored micro-seismic events and corresponding fracture parameters of each stage.

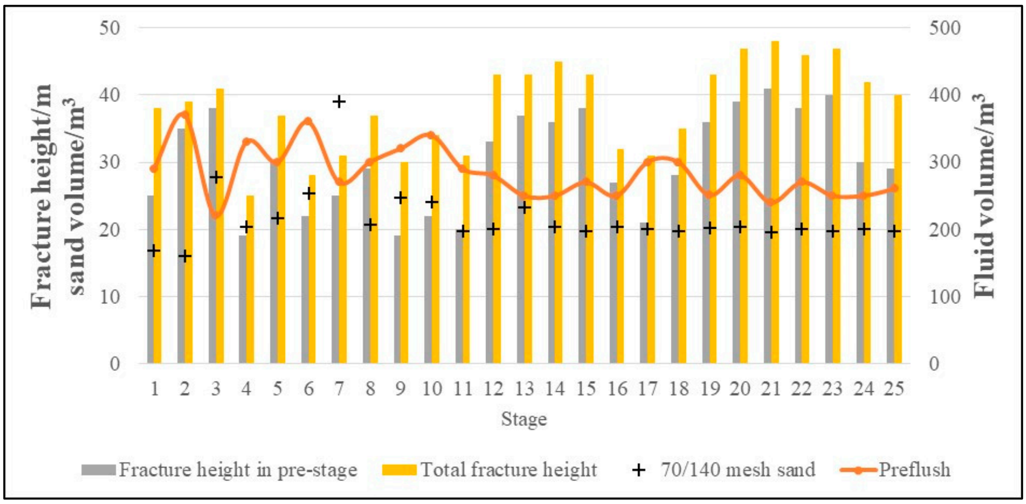

Figure 11. The effect of preflush and quartz sand on fracture propagation.

The power sand used in the pre-stage usually has a certain polishing and filtration-reducing effect, which helps to improve the permeability and fracturing effect of fracturing fluid. Through statistical analysis, it can be seen that if the amount of power sand exceeds 20 cubic meters, the polishing and filtration reduction effect can be achieved, which has guiding significance for subsequent fracturing design.

3.4. Effect of Temporary Plugging

Temporary plugging and diverting is a widespread concept that has recently been used in multi-stage fracturing of horizontal wells. It can be mainly divided into temporary plugging within hydraulic fractures and fracture-mouth temporary plugging, with the aim of improving the complexity of the fractures and increasing the stimulated reservoir volume. In general, temporary plugging balls are mainly used to plug the perforation hole, which promotes the balanced propagation for multiple clusters of fractures within the segment. The temporary plugging agent is mainly used for temporary plugging within the hydraulic fractures, promoting the turning and propagation of single-cluster fractures.

Due to the pressure limitation of the wellhead, some stages have not implemented temporary plugging processes. As shown in Figure 12, an increase in operation pressure and micro-seismic monitoring was observed after using temporary plugging balls and particles for some stages. It can be seen that the pressure rise range of the temporary plugging ball is between 1.32 MPa and 5.5 MPa, while that of the temporary plugging particles is between 0.5 MPa and 6.33 MPa. Evidently, both the plugging balls and particles achieved the favorable plugging effect. Moreover, due to the relatively small number of micro-seismic events in the first nine and the last five stages, relatively few micro-seismic events were formed after temporary plugging. However, there were significantly more micro-seismic events after temporary plugging for stages 11 to 17. Some events appear in the distance of the well trajectory, indicating that temporary plugging has the effect of increasing fracture complexity.

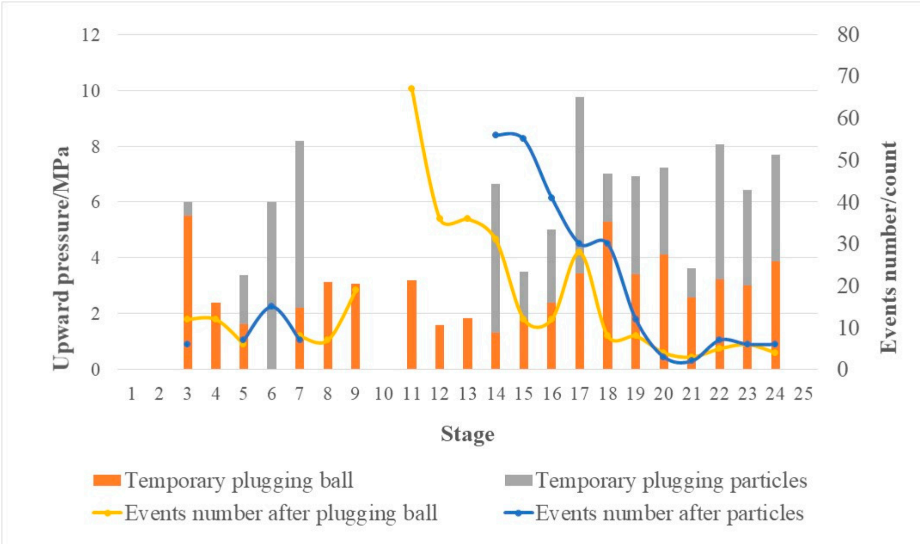

Figure 12. The effect of preflush and quartz sand on fracture propagation.

Both the incensement of wellhead pressure and micro-seismic events indicate that temporary plugging has achieved a favorable stimulation effect. In Figure 13, the distribution of micro-seismic events before and after temporary plugging using balls and particles is demonstrated. The results reveal that the micro-seismic events mainly occur in the previously stimulated area following temporary plugging with particles. Although some events do propagate to the distal ends of both sides, the propagation extent is not significant. In contrast, for temporary plugging with balls, the micro-seismic events not only appear in the previously stimulated area but also propagate to the far ends of both sides. This approach enhances the complexity of fractures and facilitates the balanced propagation of multiple clusters of fractures within the segment. Consequently, temporary plugging with balls proves to be a more effective approach in enhancing fracture complexity and promoting the balanced propagation of multiple fracture clusters compared to temporary plugging with particles.

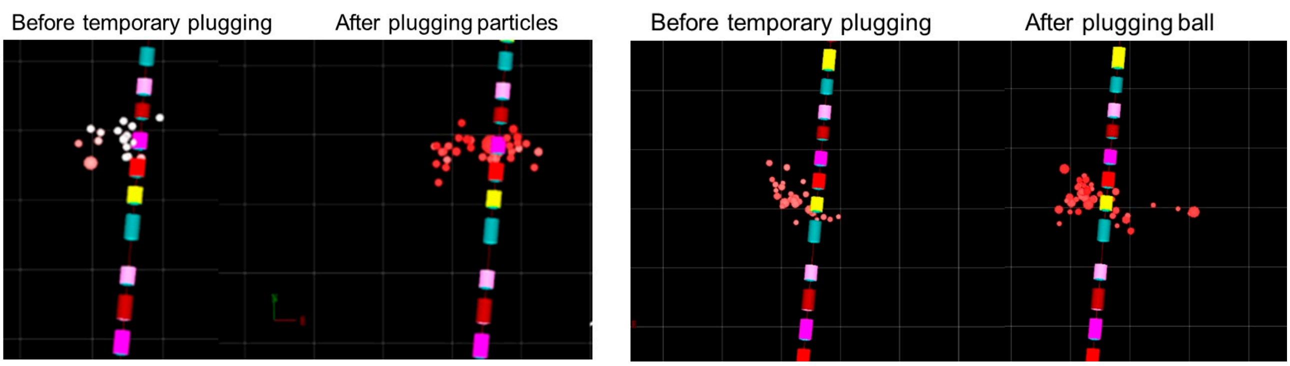

Figure 13. Micro-seismic events distribution before and after temporary plugging.

3.5. Fracture Complexity

The complexity of artificial fractures during hydraulic fracturing is mainly affected by three factors, including rock mechanics properties of the formation, crustal stress, and fracturing fluids performance. In general, complex fracture networks are the goal of hydraulic fracturing, which largely determines the stimulation effect. Micro-seismic technology is commonly used to monitor the generation and propagation of fractures and the stress state of underground rocks during hydraulic fracturing. By analyzing micro-seismic event points, the complexity of hydraulic fractures can be preliminarily determined. Specifically, the location, quantity, frequency, size, and other parameters of micro-seismic event points can provide important information about fracture complexity.

As shown in Figure 14, adjacent micro-fractures with similar fracture orientations are connected together, and isolated micro-fractures are eliminated to establish an effective micro-fracture grid for micro-seismic events of well X. In general, a complex fracture network is defined as one where the effective micro-fracture grid covers 85% of the range of micro-seismic event coverage. A moderately complex fracture network is characterized by an effective micro-fracture grid that covers 60% of the range of micro-seismic event coverage. A fracture network is considered not complex when its effective micro-grid covers less than 60% of the range of micro-seismic event coverage. Furthermore, the fracture network that developed during stages 13 and 15 was primarily influenced by the presence of existing natural fractures near faults. The fracture network that resulted from hydraulic fracturing in the stage away from the fault is generally not complex. This implies that geological conditions are a prerequisite for creating a complex network of fractures and that only engineering techniques can facilitate the appropriate enhancement of fracture complexity.

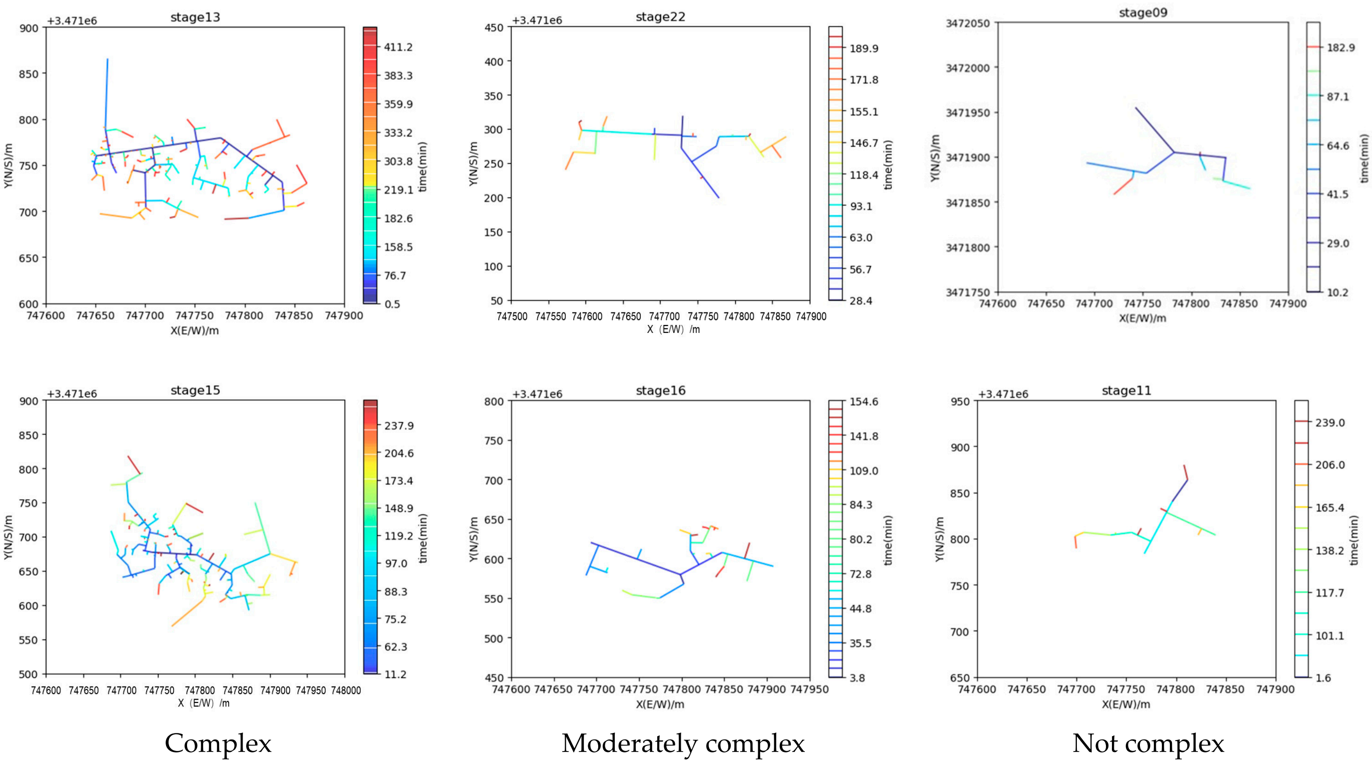

Figure 14. Fracture complexity for different stages.

4. Conclusions

In this paper, we first introduced the basic parameters of well X, including porosity, gas-bearing properties, mineral composition, rock mechanics parameters, and crustal stress.

Then, the post-fracturing evaluation for well X was performed on the basis of micro-seismic monitoring. The following conclusions and application prospects can be reached:

(1) The target well X exhibits characteristics such as low porosity and permeability, high gas-bearing content, low concentration of clay minerals, high modulus, high compressive strength, and moderate horizontal stress difference.
(2) The correlation between the number of micro-seismic events and the fracture size is relatively poor under the condition of high fluid strength. That is to say, the fracture size is essentially formed when the fluid volume exceeds a certain level.
(3) Cross-linked slickwater with high viscosity and the amount of power sand exceeding 20 cubic meters can satisfy the polishing and filtration reduction effect, which is conducive to the propagation of the fracture height.
(4) Temporary plugging balls facilitate the balanced propagation of multiple fracture clusters within a stage, whereas temporary plugging particles promote the formation of complex fractures.
(5) Geological conditions are a prerequisite for creating a complex network of fractures, and only engineering techniques can facilitate the appropriate enhancement of fracture complexity.
(6) Micro-seismic technology can be applied in the fracturing of unconventional oil and gas reservoirs such as shale oil reservoirs, which can enable commercial productivity.

Author Contributions: Conceptualization and methodology, L.Z.; resources, H.W.; data curation, J.C.; supervision, S.Z. All authors have read and agreed to the published version of the manuscript.

Funding: This work was financially supported by the China Petroleum and Chemical Corporation (Grant No. P21063-3) and Young Elite Scientist Sponsorship Program by BAST (No.BYESS2023016).

Data Availability Statement: Not applicable.

Acknowledgments: This work was financially supported by the China Petroleum and Chemical Corporation (Grant No. P21063-3).

Conflicts of Interest: The authors declare no conflict of interest.

References

1. EIA. *Annual Energy Outlook 2018*; U.S. Energy Information Administration: Washington, DC, USA, 2022.
2. Zhang, L.; Zhou, F.; Mou, J.; Xu, G.; Zhang, S.; Li, Z. A new method to improve long-term fracture conductivity in acid fracturing under high closure stress. *J. Petrol. Sci. Eng.* **2018**, *171*, 760–770. [CrossRef]
3. Zhang, L.; Zhou, F.; Zhang, S.; Li, Z.; Wang, J.; Wang, Y. Evaluation of permeability damage caused by drilling and fracturing fluids in tight low permeability sandstone reservoirs. *J. Petrol. Sci. Eng.* **2019**, *175*, 1122–1135.
4. Zhang, L.; Zhou, F.; Mou, J.; Pournik, M.; Tao, S.; Wang, D.; Wang, Y. Large-scale true tri-axial fracturing experimental investigation on diversion behavior of fiber using 3D printing model of rock formation. *J. Petrol. Sci. Eng.* **2019**, *181*, 106171. [CrossRef]
5. Zhang, L.; Zhou, F.; Mou, J.; Feng, W.; Li, Z.; Zhang, S. An integrated experimental method to investigate tool-less temporary-plugging multistage acid fracturing of horizontal well by using self-degradable diverters. *SPE J.* **2020**, *25*, 1204–1219. [CrossRef]
6. Zhuang, Z.; Liu, Z.L.; Wang, T.; Gao, Y.; Wang, Y.H.; Fu, H.F. The key mechanical problems on hydraulic fracture in shale. *Chin. Sci. Bull.* **2016**, *61*, 72–81. [CrossRef]
7. Bing, H.; Zhi, C.; An'an, W.; Derek, E. Simulation of competitive propagation of multi-fractures on shale oil reservoir multi-clustered fracturing in Jimsar sag. *Acta Pet. Sin.* **2022**, *43*, 75–90.
8. Rassenfoss, S.; Zborowski, M. Hydraulic fracturing:Fracturing plans and reality often look really different. *J. Pet. Technol.* **2018**, *70*, 30–41. [CrossRef]
9. Ugueto, C.; Huckabee, P.; Molenaar, M.; Brendan, W.; Kiran, S. Perforation cluster efficiency of cemented plug and Perf limited entry completions: Insights from fiber optics diagnostics. In Proceedings of the SPE Hydraulic Fracturing Technology Conference, The Woodlands, TA, USA, 9–11 February 2016; SPE: The Woodlands, TA, USA, 2016. SPE-179124-MS.
10. Sui, W.; Wen, C.; Sun, W. Joint application of distributed optical fiber sensing technologies for hydraulic fracturing monitoring. *Nat. Gas Ind.* **2023**, *43*, 87–103.
11. Zhao, C.; Wang, H.; Guo, W.; Zhang, W.; Fan, Q.; Tian, J.; Zhao, J. Microseismic monitoring technology of shale gas pressure fracture: A case study from X platform in Weiyuan area of Sichuan Basin. *Prog. Geophys.* **2022**, *37*, 2089–2096. (In Chinese)
12. Reshetnikov, A.; Nazarova, A.; Taylor, S.; Haffener, J.; Langton, D.; Biholar, A.; Anderson, S.; Devon Energy Corporation. Observations, Learnings, and Validation of Conductive Fracture Imaging. In Proceedings of the SPE Hydraulic Fracturing Technology Conference and Exhibition, The Woodlands, TA, USA, 31 January–2 February 2023.

13. Bosikov, I.I.; Klyuev, R.V.; Mayer, A.V. Comprehensive assessment of hydraulic fracturing technology efficiency for well construction during hydrocarbon production. *J. Min. Inst.* **2022**, *258*, 1018–1025. [CrossRef]
14. Zaalishvili, V.B.; Hasanov, A.B.; Abbasov, E.Y.; Mammadova, D.N. Detailing the Pore Structure of Productive Intervals of Oil Wells Using the Color 3D Imaging. *Energies* **2023**, *16*, 217. [CrossRef]
15. Maxwell, S.; Norton, M. Enhancing shale gas reservoir characterization using hydraulic fracture microseismic data. *First Break* **2012**, *30*, 95–101. [CrossRef]
16. Refunjol, X.E.; Marfurt, K.J.; Le Calvez, J.H. Inversion and attribute-assisted hydraulically induced microseismic fracture characterization in the North Texas Barnett Shale. *Lead. Edge* **2011**, *30*, 292–299. [CrossRef]
17. Wu, F.; Yan, Y.; Yin, C. Real time monitoring technology for microseismic fracturing of shale gas: A case study in Southern Sichuan Basin. *Nat. Gas Ind.* **2016**, *36*, 46–50. [CrossRef]
18. Wang, G.Q.; Xiao, Y.J.; Zhao, H.; Wang, Y.; Chen, Y. Application of microseis-mic monitoring technology to re—Fracturing of shale gas horizontal wells. *Geol. Explor.* **2019**, *55*, 1336–1342.
19. Zhao, C.; Zhang, W.; Tian, J.; Mo, G.; Ren, L.; Cheng, Z.; Li, J.; Zhao, J.; Xu, H. Adjustment and effect of oilfield development plan based on microseismic monitoring technology—Taking Block J2 of Liaohe exploration area as an example. *Prog. Geophys.* **2022**, *37*, 320–327.

Disclaimer/Publisher's Note: The statements, opinions and data contained in all publications are solely those of the individual author(s) and contributor(s) and not of MDPI and/or the editor(s). MDPI and/or the editor(s) disclaim responsibility for any injury to people or property resulting from any ideas, methods, instructions or products referred to in the content.